Invited Paper Presented at: Fifth New York University Workshop on Penetration Phenomena:
Exotic Projectiles in Matter
January 8 to 10, 1981

BNL-29448

CONF-810150--1

COULOMB EXPLOSION OF LARGE PENETRATING MOLECULAR CLUSTERS

H.E. Wegner and P. Thieberger

I. INTRODUCTION

The sputter ion source[1] of the Tandem Van de Graaff accelerator facility at Brookhaven National Laboratory is used to provide negative ions of many elements and compounds throughout the entire Periodic Table for the study of heavy ion nuclear physics. The sputter ion source accelerates positive cesium ions to any energy of 20 to 30 kV and then impinges them upon some surface out of which the cesium ions sputter either elemental negative ions or in many cases molecular negative ions of many kinds. A mass distribution of the negative ions sputtered from the surface of graphite is shown in Fig. 1. The designated mass peaks in the figure correspond to C_n^- for n=1-12. It is interesting to note that the mass 6 and 8 carbon molecules are more intense than their odd neighbors, 5 and 7, which could indicate that they include a contribution from carbyne structures which are hypothesized to be a one dimensional form of carbon that is sometimes formed in the process of making graphite and are also found in carbonacious meteorites.[2]

The main purpose of these Coulomb explosion measurements is to determine what kind of structure these and other complex molecules may have and also to determine what other special phenomena may come into play as these complex molecules pass through matter. Although the first preliminary measurements involving the Coulomb explosion of these molecules was reported at this workshop last year, the results will be briefly summarized before going on to the more recent measurements[4] obtained with a completely new kind of detector system.[5]

The experimental arrangement for these initial studies is shown in Fig. 2. The experiments were all carried out with the first large Tandem accelerator of the two machines comprising the Tandem Van de Graaff Facility. This machine is used as an injector for the second machine, approximately half of the operating

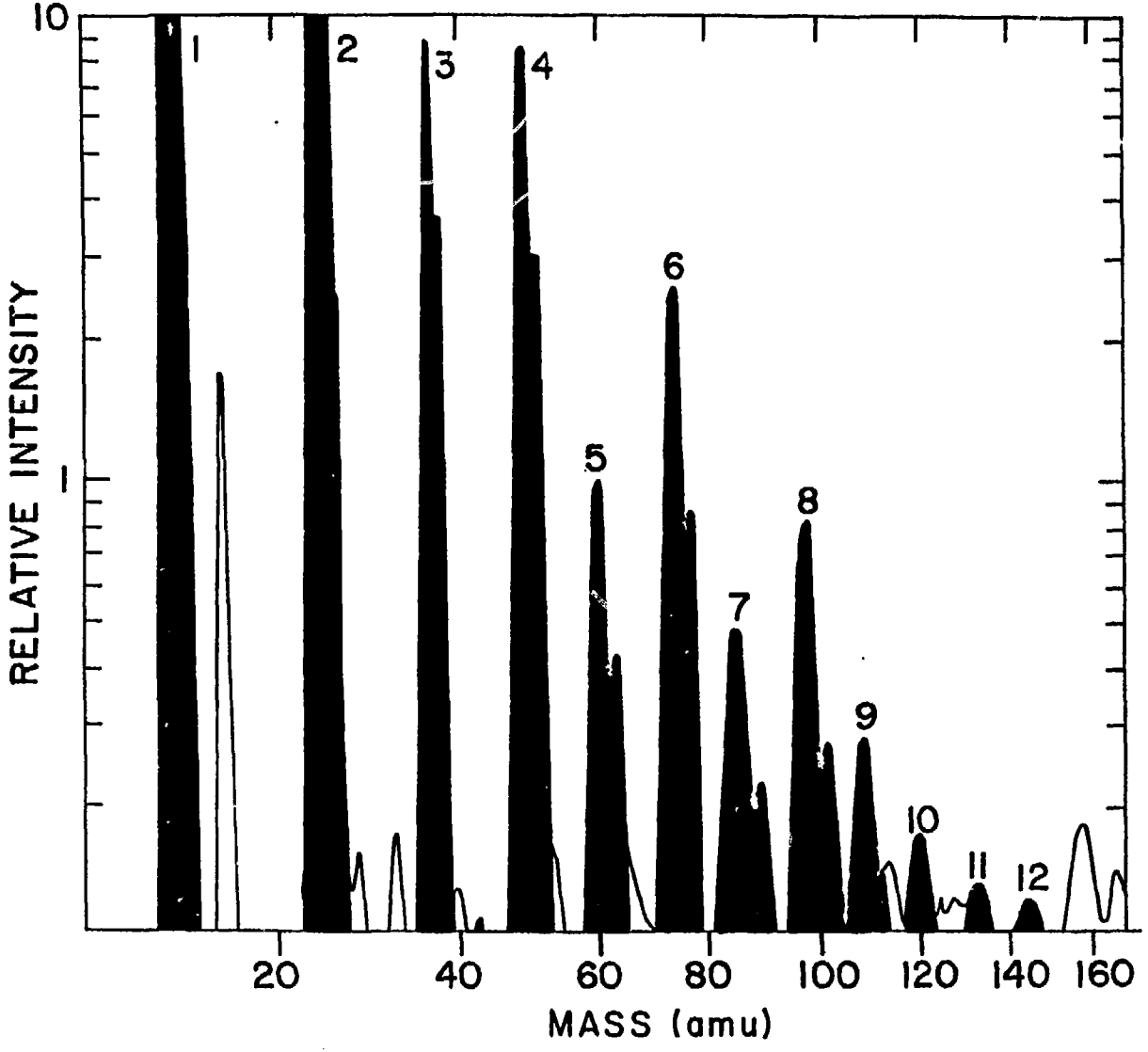

Figure 1. Mass spectrum for Cs sputter negative ion source operating with a carbon cone.

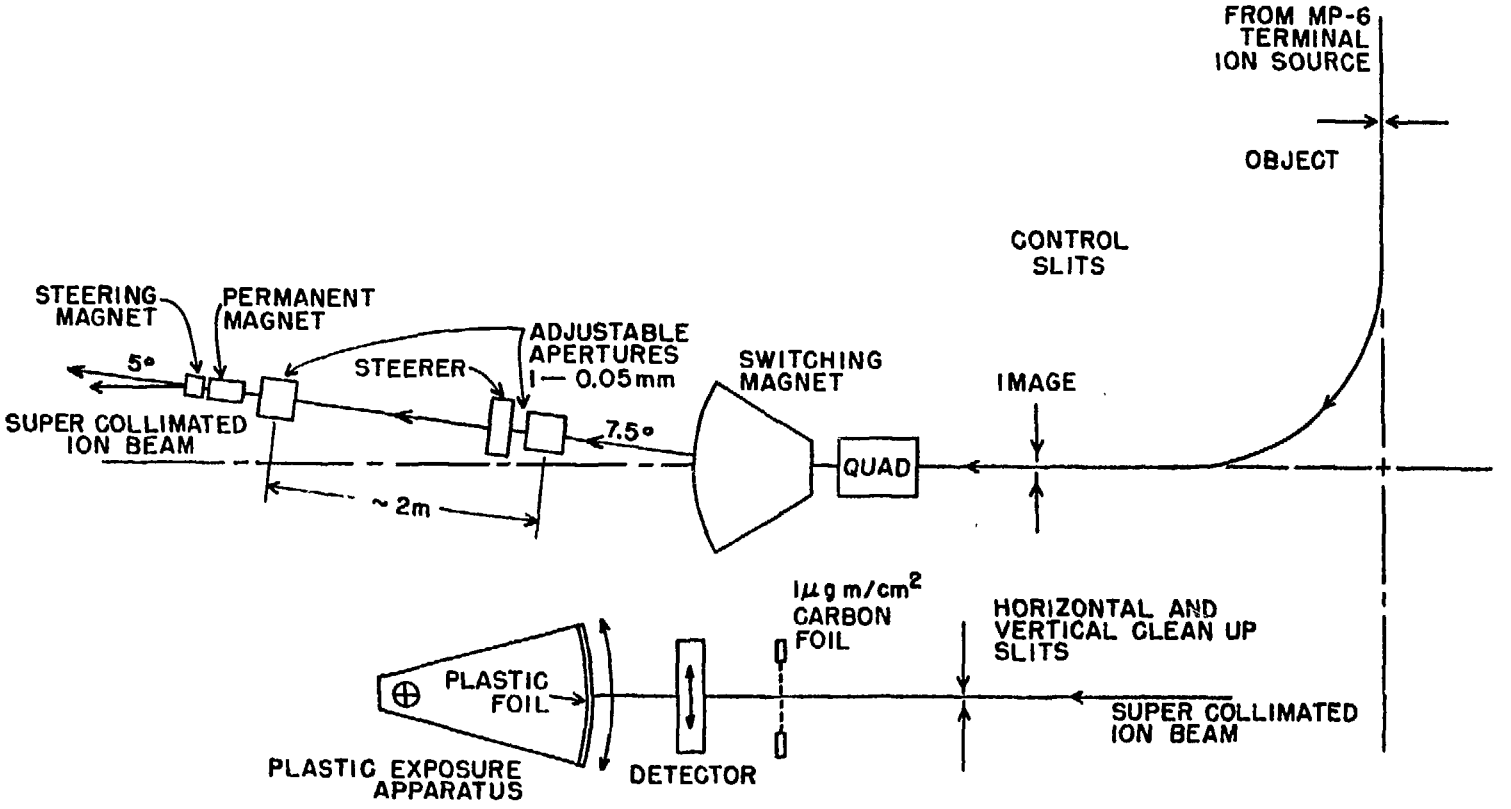

Figure 2. Experimental arrangement for Coulomb explosion measurements utilizing a polycarbonate track detector. (see text)

time of the facility, and is available for other kinds of experiments when not being used as an injector. It also happens to be the largest accelerator in the world containing a terminal negative ion source which allows the study of negative ions, produced in the source, accelerated to ground and then transported to the apparatus as shown in Fig. 2. Similarly, the negative ions can also be accelerated through the Tandem after being injected from an external ion source; they are then exchanged to positive ions by collision in a small amount of gas inside the high voltage terminal and exit from the machine as positive ions. This convenient arrangement allows most of these molecular ions to be studied either as positive or negative ions. Since the ions can be charge exchanged relatively easily in gas, it may even be possible in the future with this particular apparatus to do some limited studies with the neutral molecule as well.

The positive or negative molecular ions emerging from the accelerator are magnetically analyzed for proper identification and then transported through a series of magnets and adjustable tiny apertures until they proceed to a stripper foil made of 1 $\mu g/cm^2$ self-supporting carbon. As the MeV energy molecular ions pass through the thin carbon stripping foil, they are suddenly stripped to an average charge state of approximately 2.5 charges, and strongly repel each other with several tens of electron volts of energy. The plastic polycarbonate foil is distant enough so that the particles spreading from the consequences of Coulomb repulsion are conveniently separated when they impinge on the plastic foil. Particle intensity is arranged to be a few particles per second, and the plastic foil is mechanically moved back and forth as indicated in the figure as well as up and down, so as to cover most of the foil with Coulomb explosion events. After exposure, the foil is electrically etched to show the relative coordinates of the impinging atomic components of the

original molecule. A photograph of a developed polycarbonate foil approximately five times normal size is shown in Fig. 3. Unfortunately, the beam intensity cannot be controlled to a uniform few particles per second, and instead, occasional bursts of large numbers of molecules go into the detector foil. These intense burst areas can be observed on the slide as well as a number of individual triangular events due to the Coulomb explosion of C_3^- ions which were used for this particular exposure.

A further enlargement of C_3^- events is shown in Fig. 4 and it is observed that the characteristic signature of the carbon ions after development is the ragged edge circular event that differentiates the carbon ions from miscellaneous background spots and debris. The very close triangular grouping in the lower right hand corner of Fig. 4 corresponds to a molecule that was broken up by a gas collision but without ionizing the atomic components. The usual charge state received in passing through the stripping foil then produces little or no Coulomb explosion because the atomic components had sufficiently separated from the loss of molecular binding. Figure 5 is a microscopic view of the Coulomb explosion of the NCO molecule and triangular-like events are observed. With this detector system there is no way to differentiate between the C, N and O atomic components of the molecule.

With a set of triangular-like data of this kind, the experimental question is whether these triangles represent an initial structure corresponding to a triangular or linear bonded molecule that is in some kind of bending oscillation mode as indicated in Fig. 6. The breathing mode does not have to be considered because it is simply a transformation of a rod-like system to another rod-like system, with different spacing between the molecular components. On the other hand, the bending mode forms triangles of varying sizes and shapes depending on

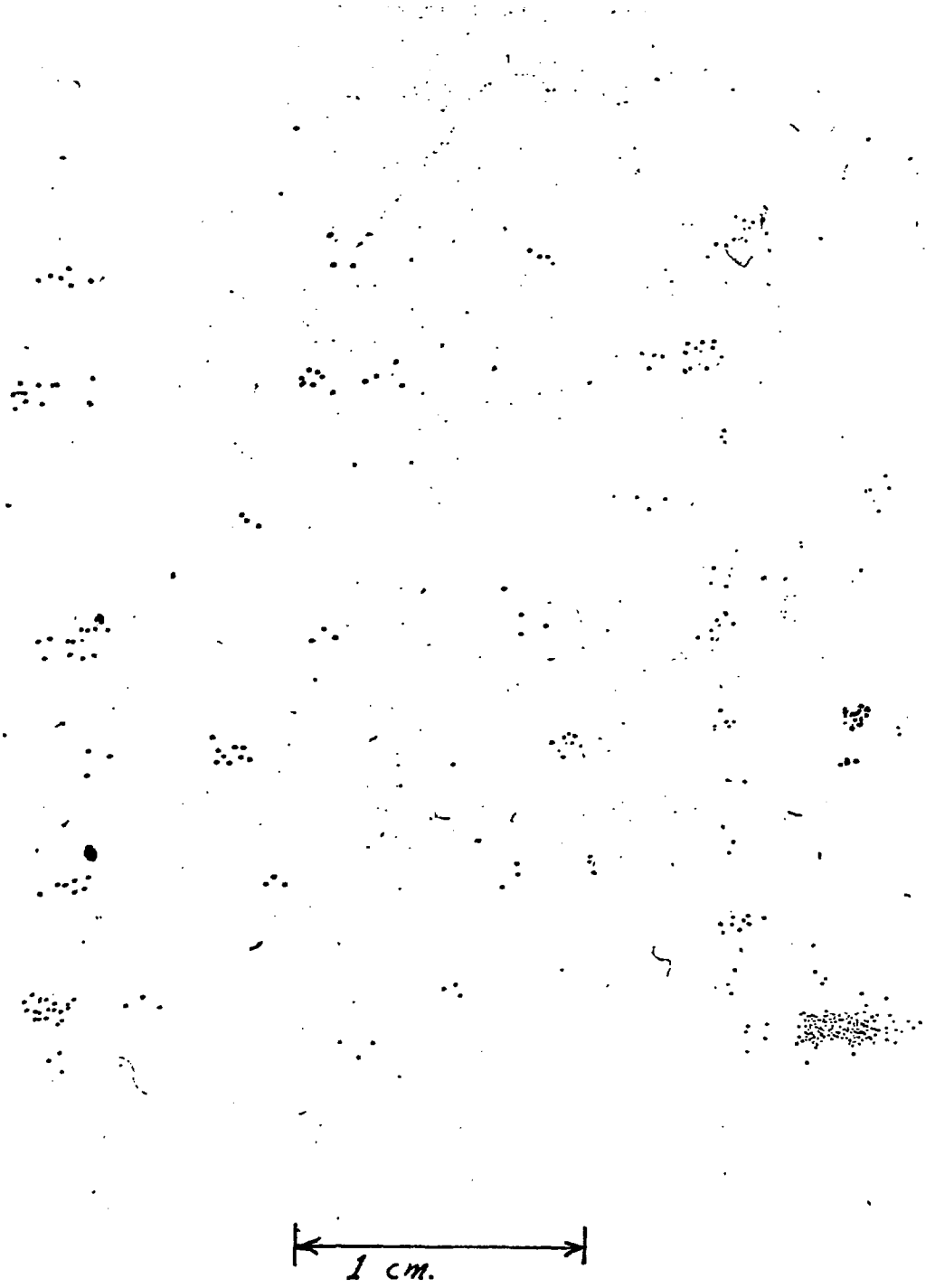

Figure 3. Electroetched polycarbonate foil after exposure to C_3^- ions that have been Coulomb exploded.

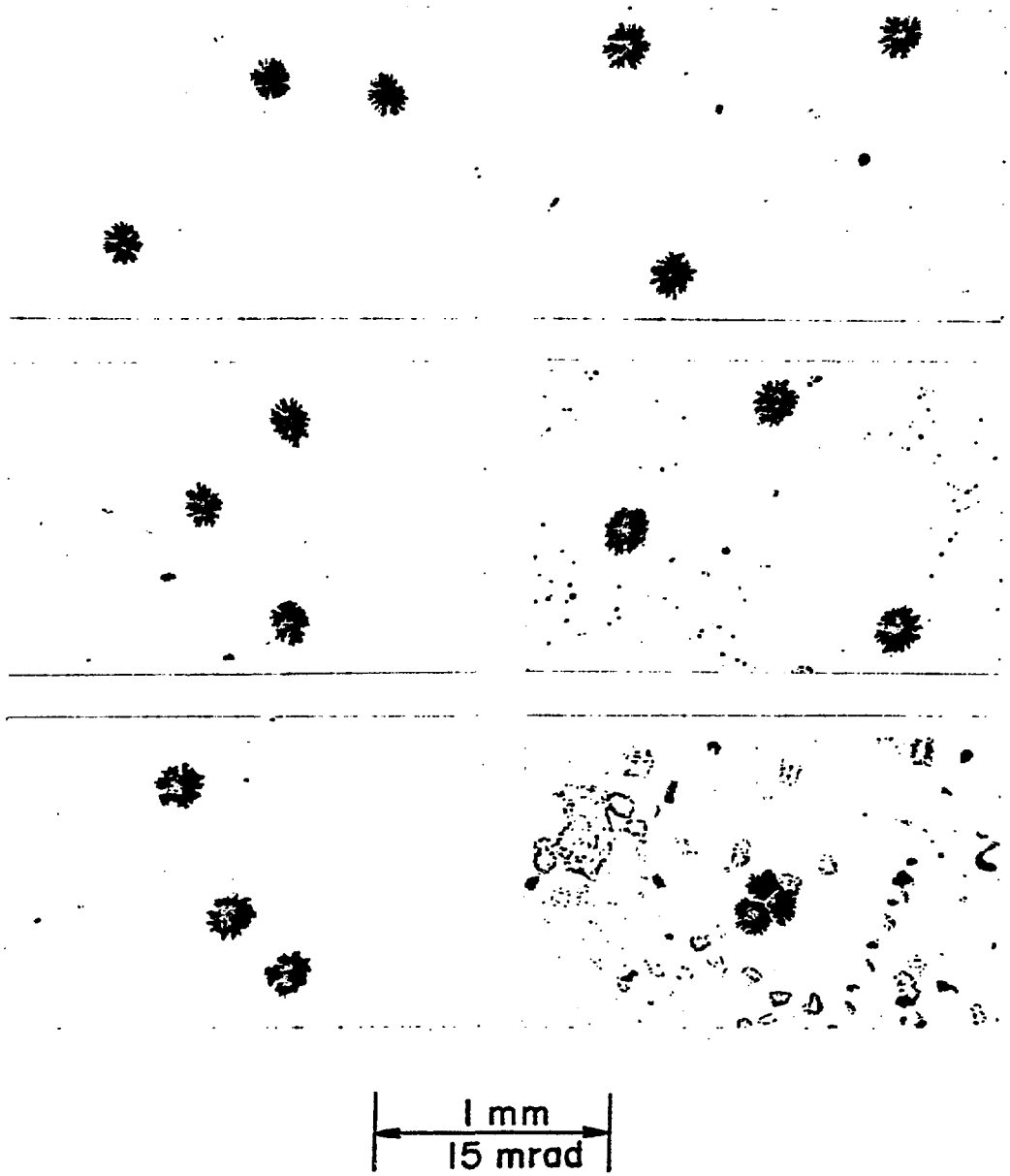

Figure 4. Photomicrographs of Coulomb exploded 4.67 MeV C_3^- ions.

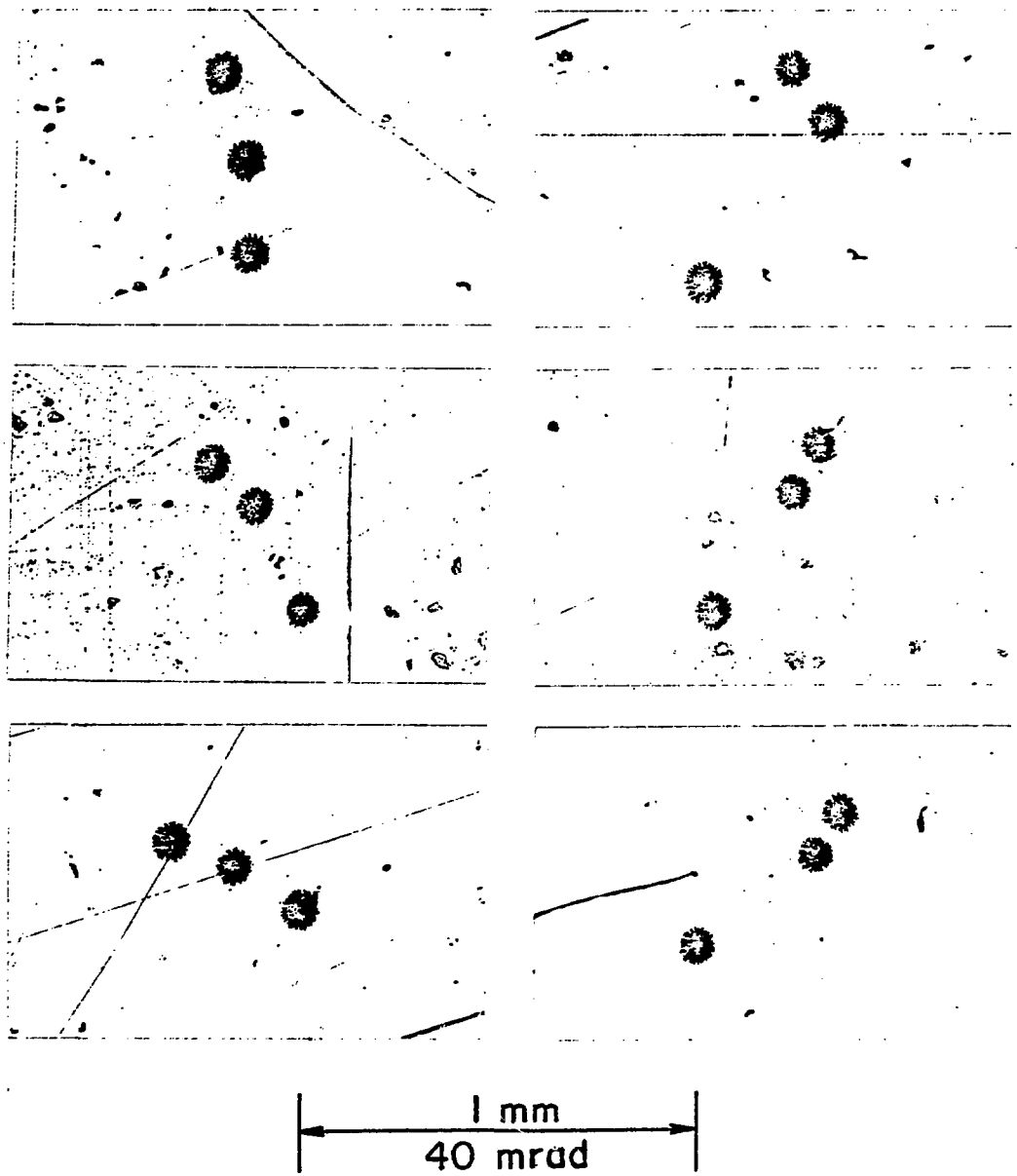

Figure 5. Photomicrographs of Coulomb exploded 4.00 MeV NCO^- ions.

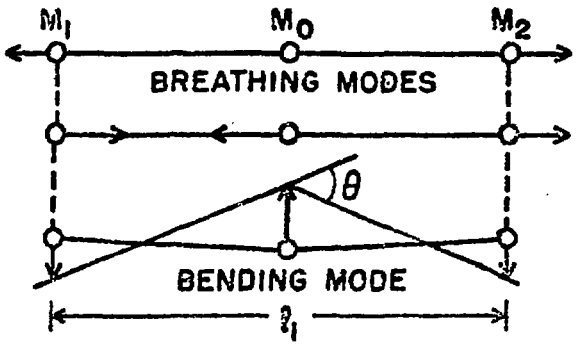

Figure 6. Bending and breathing modes of vibration for a rod-like triatomic molecule.

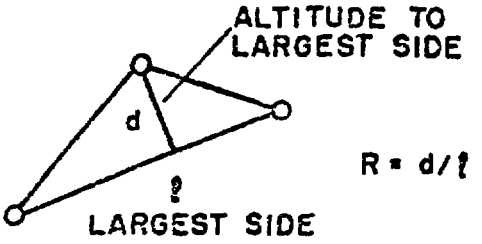

Figure 7. Triangle parameters for a triatomic Coulomb explosion event.

when the particular Coulomb explosion occurs.

The resulting triangle events can be analyzed in terms of the longest side of the triangle, l, and the ratio of the altitude of the triangle in respect to that side, d, as shown in Fig. 7. The experimental problem now has to do with the fact that these original unexploded molecular structures are randomly oriented in any particular orientation in respect to the beam direction or the plane of the stripping foil. Consequently, any theoretical model of the final distribution of triangles must include the random orientation. In addition, the Coulomb explosion tends to distort any initial triangular structure toward an equilateral shape as indicated in Fig. 8. This figure shows that molecular triatomic triangular-like structures with an initial angle varying from approximately 40 to 120 degrees, will all emerge from the stripping foil as approximately equilateral triangles. To further complicate matters, none of the atoms necessarily have the same charge state as assumed in the figure. The charge state varies from 1^+ to 4^+ with an average charge state of approximately 2.5^+. The different charge states of the different atoms distort the Coulomb explosion even further, and these effects must also be folded into the theoretical calculation that is stimulating the Coulomb explosion.

Analysis of the triangles observed for several different Coulomb explosion systems of approximately 5 MeV energy is shown in Fig. 9. In this analysis the ratio of the height of the triangle to the longest side or d/l ratio is plotted in a 16 x 16 two dimensional ray as a function of l. With these very limited statistics, a striking similarity can be observed between the NCO^- and NCO^+ data, as well as a noticeable difference for the C_3^- distribution. The fact that the centroid of the C_3^- distribution is at a smaller l than either the NCO^- or NCO^+ data, means that the Coulomb explosion for the C_3^- molecule was not as

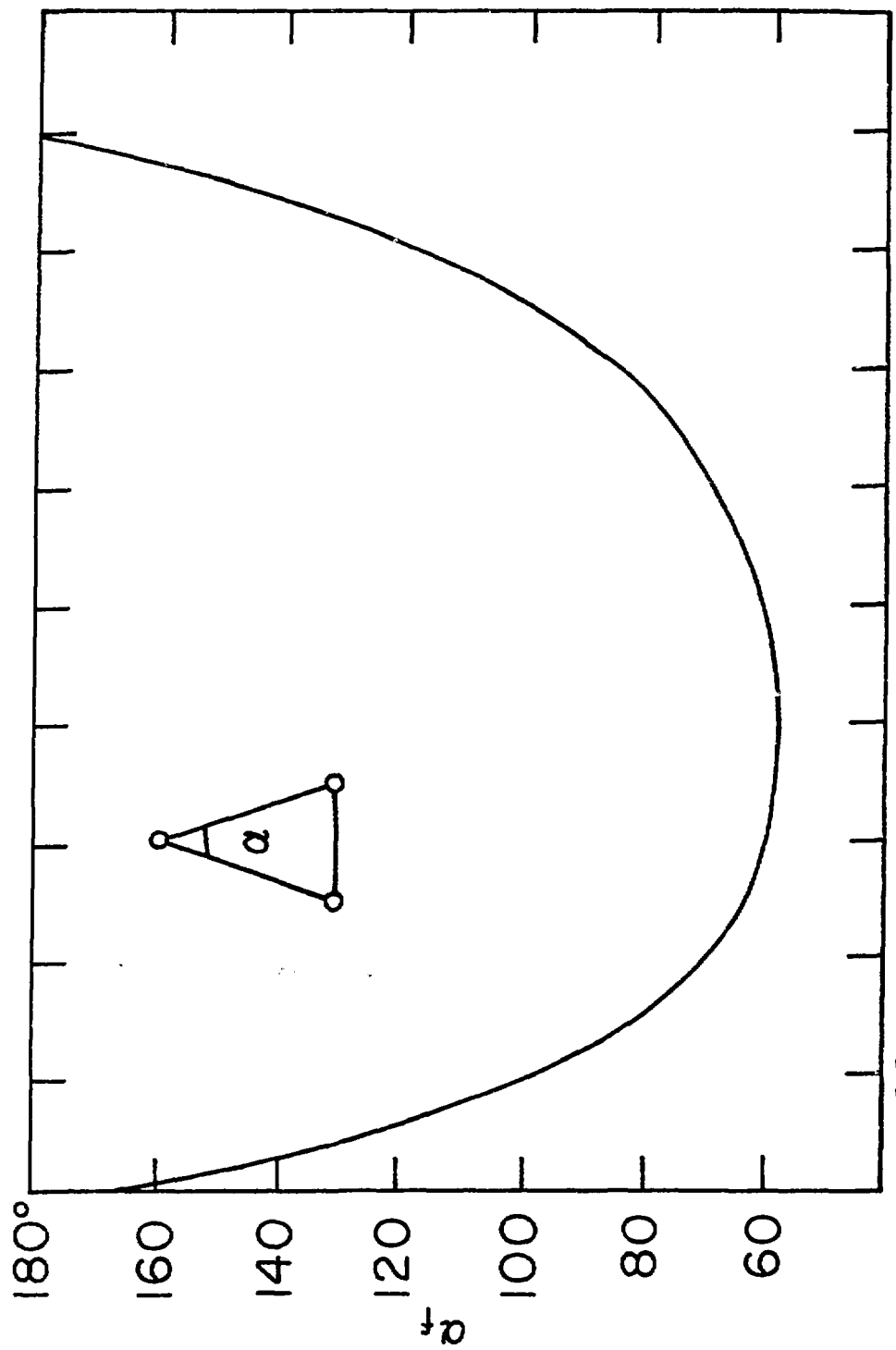

Figure 8. Initial angle vs. final angle for a triatomic molecule before and after undergoing a Coulomb explosion.

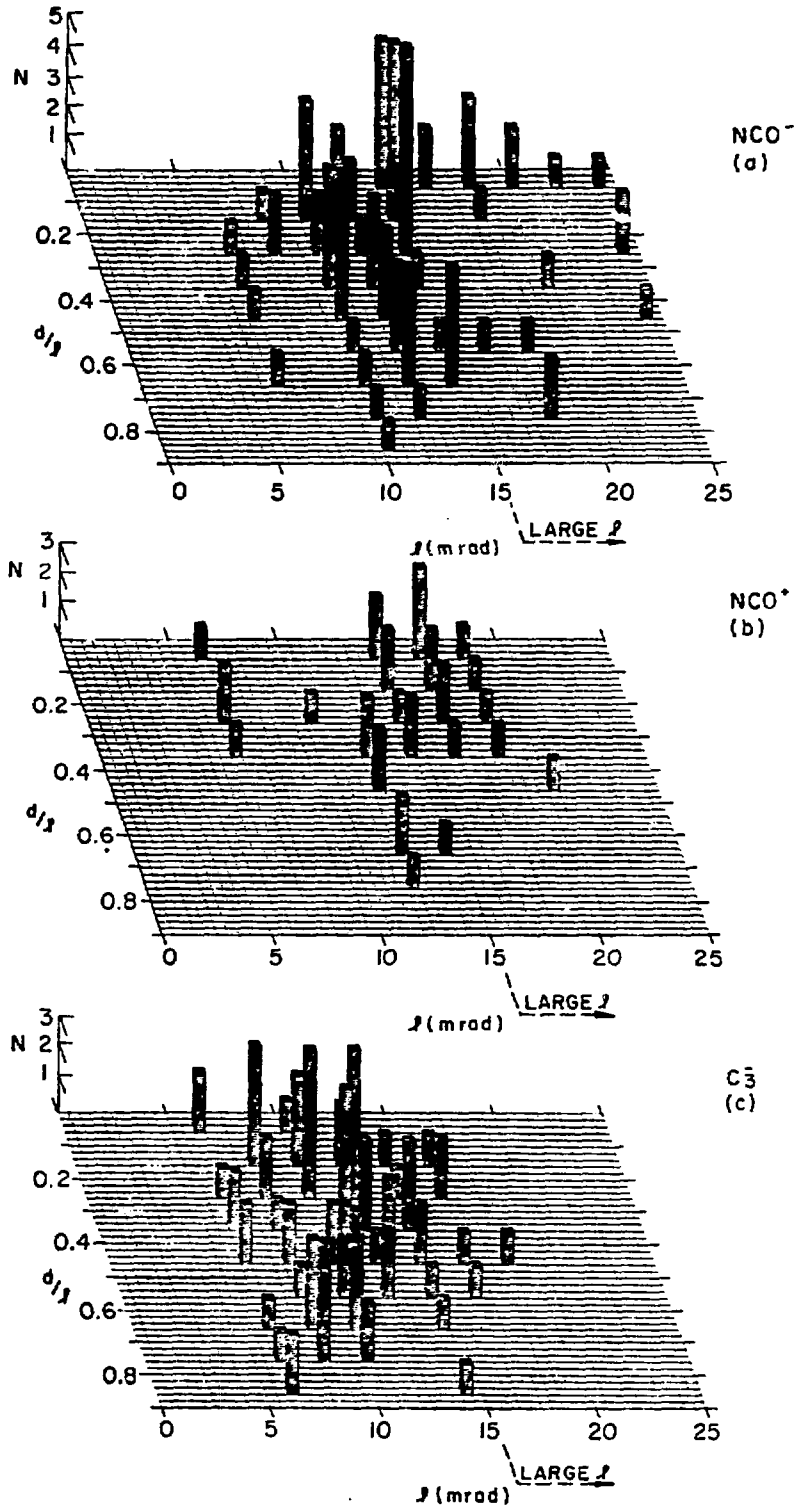

Figure 9. Experimental distributions of triatomic Coulomb explosion events for 4.00 MeV NCO^-, NCO^+ and 4.67 MeV C_3^- molecules plotted as a 16 x 16 array of the ratio d/l vs. l.

violent as that for the other two molecules which means that the average separation of the atomic components of the molecule must have been larger or the average charges higher. The fact that the triangular events vary over a d/l range from a straight rigid rod configuration, (d/l = 0) to an equilateral triangle configuration, (d/l = .86) means that a specific assignment of detailed molecular shape will require more detailed statistics than is possible with this original polycarbonate method.

A further complexity to the analysis of the scattering process is from the multiple scattering of the atomic components as they pass through the very thin foil. The multiple scattering process results in the particle's trajectory not being exactly determined by the Coulomb explosion, but being perturbed by short and long range collisions with some of the carbon atoms as the ion penetrates the carbon foil. This means that the Coulomb explosion pattern is partially blurred by this phenomenon. In order to show the effects of multiple scattering on this kind of analysis, Fig. 10 shows the results of theoretical calculations involving the Coulomb explosion of a triangular-like C_3^- structure. In this calculation, the varying charge states of the different ions were folded in, as well as all of the random orientations assuming an initial triangular-like structure. The ridge-like distributions observed for the "no-multiple scattering" case at the top of the figure represent different charge state combinations of the three ions that make up the C_3^- molecule. Multiple scattering occurs during the fraction of the Coulomb explosion taking place inside the foil. To simplify the calculations two different approximations were used. First, the multiple scattering was presumed to occur before the Coulomb explosion, and under these conditions a large amount of the non-scattering structure is retained as indicated in the figure. The other extreme is for the multiple scattering to occur after the Coulomb ex-

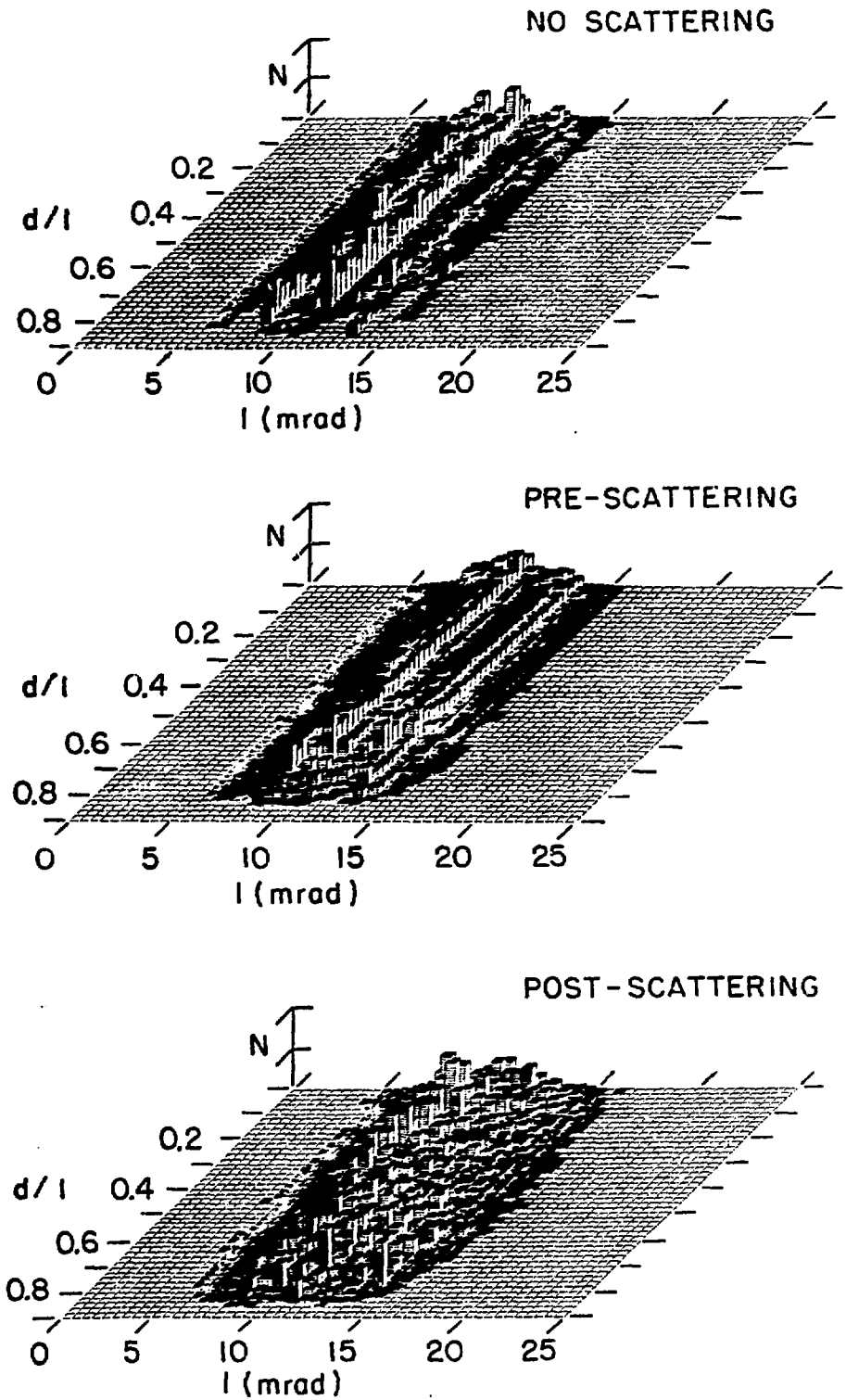

Figure 10. Theoretical calculations corresponding to a triangular C_3 molecule undergoing a Coulomb explosion a) without multiple scattering b) with multiple scattering before the Coulomb explosion c) with multiple scattering after the Coulomb explosion.

plosion as shown in the bottom of the figure, and it is observed that most of the structure due to the charge state configuration is largely obliterated by the multiple scattering. On the other hand, there is some structure in the form of a gradual curve.

Figure 11 shows the kind of distribution that would be observed with an oscillating bending rod-like structure in the lowest n=0 state, as well as a much higher n=6 excited state including the effects of post multiple scattering. The upper figure corresponds to n=0 and shows that the triangle distribution is largely obtuse triangles with many rod-like structures having a d/l ratio equal to 0. On the other hand, when the rod-like structure oscillates with considerable amplitude as shown in the lower figure for n=6, the small d/l ratio events are relatively suppressed and instead, a distribution of events over most of the two dimensional plane is observed. Although these results are different from the theoretical predictions of a triangular-like structure, they are similar enough to indicate that very good statistics data must be taken in order to determine what kind of specific structure the original molecule might have.

II. Two Dimensional Image Intensifier Detector System

The idea behind the 2D Image Intensifier Detector System is to replace the polycarbonate foils shown in Fig. 2 with a suitably located thin phosphor screen that will scintillate when struck by the incident heavy ions from the Coulomb explosion. This thin phosphor screen[6] is deposited on the entrance fibre optic plate of a commercially available image intensifier.[7] The image intensifier provides a light gain of 85,000 and maintains the relative spacial location of the scintillations produced in the phosphor by the energetic ions. A schematic diagram of the image intensifier is shown in Fig. 12. This unit is a three-stage

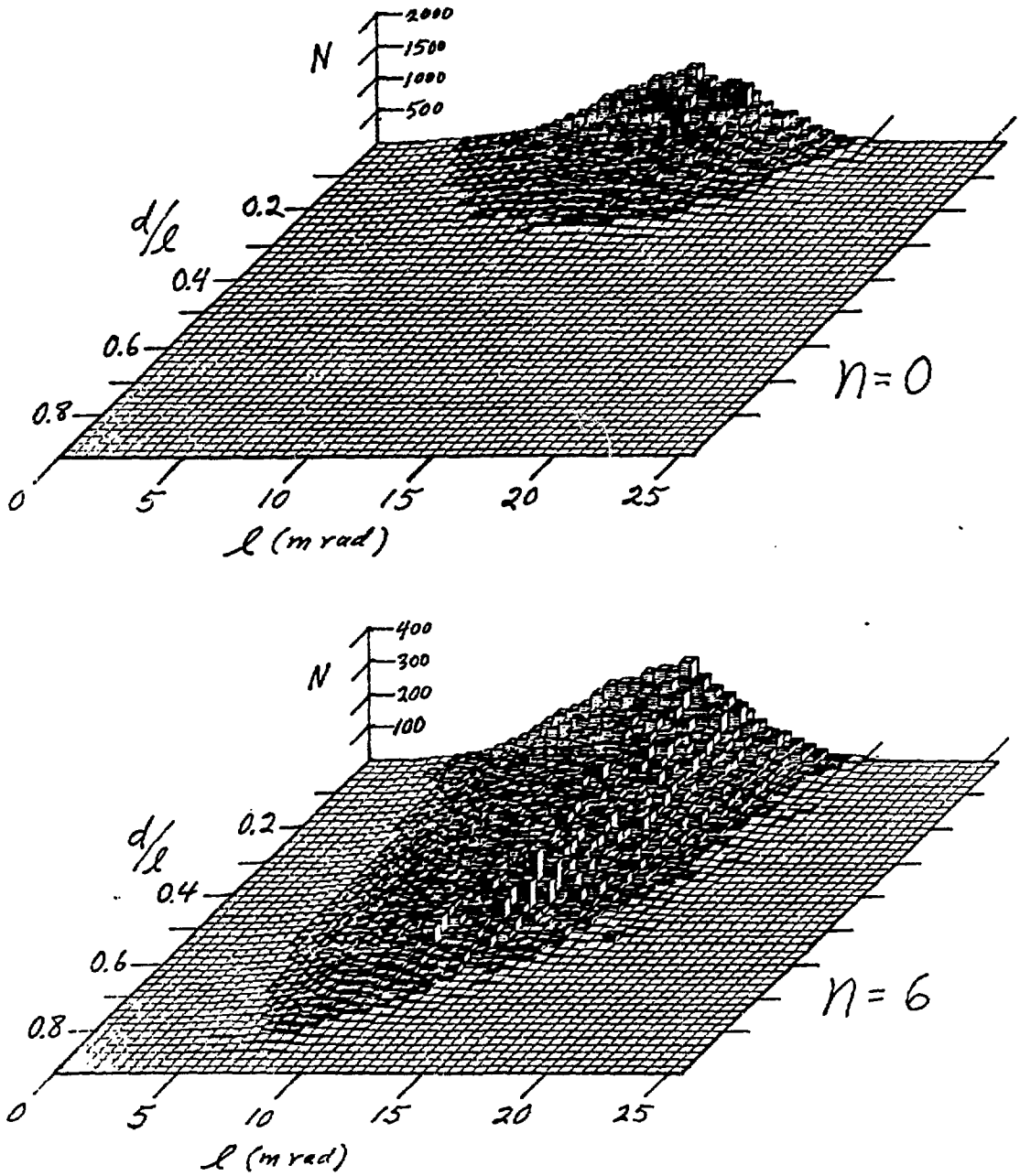

Figure 11. Theoretical calculations corresponding to a rod-like C_3 molecule vibrating in a bending mode and undergoing a Coulomb explosion a) lowest order vibration, N=0 b) N=6.

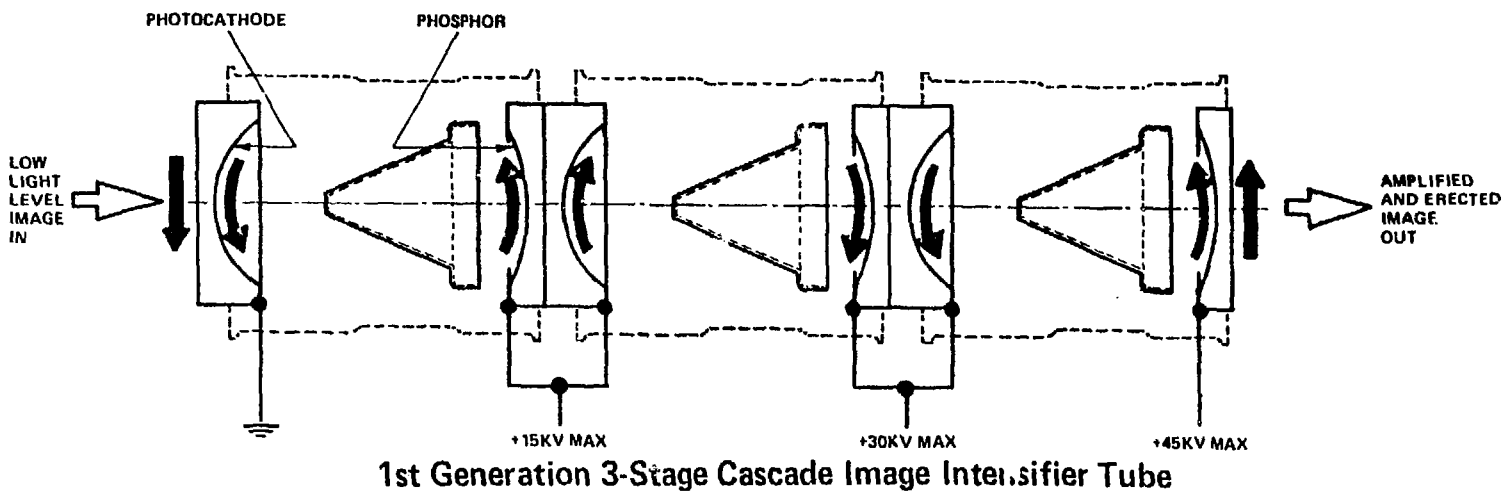

Figure 12. Schematic diagram of three stage image intensifier (by permission of Varo Electron Devices Inc.).

amplifier consisting of three separate image intensifiers cascaded together as shown in the schematic. Each state operates at 15 kV which means that the output fibre optic plate is at 45 kV above ground and must have a special fibre optic extension plate 25 mm long, that is optically coupled and sealed to the rest of the assembly in order to electrically isolate the final high voltage stage from the outside world so as to eliminate corona sparking and other undesirable high voltage phenomena. Figure 13 shows the three assembled stages as well as their final assembly with included power supplies inside a plastic housing. Figure 14 is a closeup photograph of the output extension plate showing the amplified scintillation light spots produced by 5 MeV alpha particles impinging at random on the phosphor coated input fibre optic plate. In operation, the image intensifier is enclosed in a simple cylindrical aluminum shell and end cap housing arranged with a 30 mm diameter hole surrounded by an O-ring which seals to the front surface of the input fibre optic plate. The base of the housing is then arranged to couple conveniently onto the vacuum system of the rest of the apparatus.

The experimental arrangement for the imaging of Coulomb explosion events is shown schematically in Fig. 15. A 1 $\mu g/cm^2$ carbon foil 60 cm in front of the image intensifier assembly serves as a stripper foil to break up and Coulomb-explode C_3^- ions accelerated to 4.67 MeV. The 60-mm flight path provides enough distance so that the particles spreading from the Coulomb explosion are conveniently separated when they impinge on the scintillation screen. The relative locations of the scintillations can then be interpreted in terms of the relative orientation and separation of the carbon ions forming the molecular structure at the moment of collision with the carbon foil.

An alpha particle source and silicon detector can be inserted on the beam line for test purposes. A calibration plate containing a number of tiny apertures

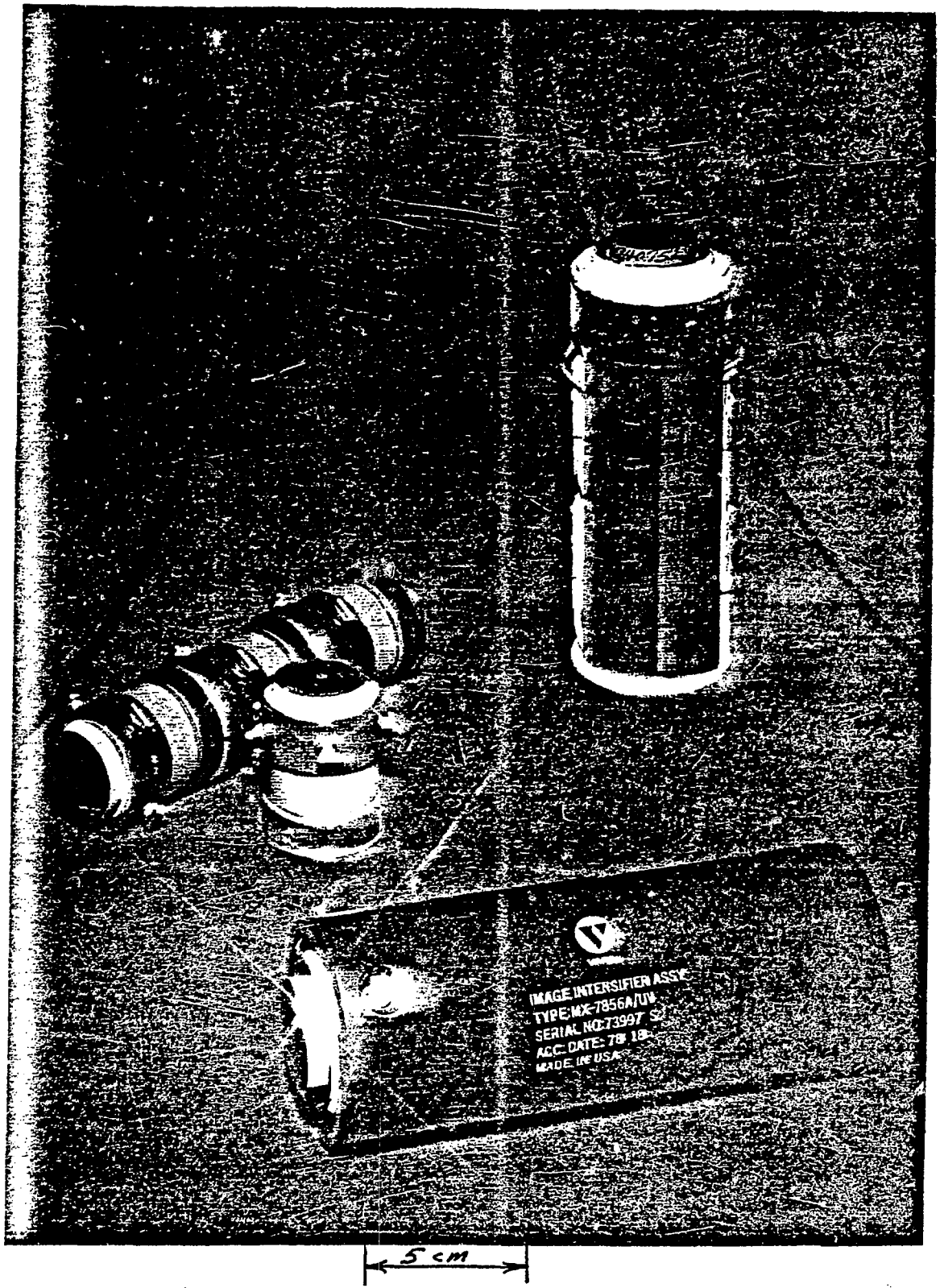

Figure 13. Three stage image intensifier before and after final assembly (by permission of Varo Electron Devices Inc.)

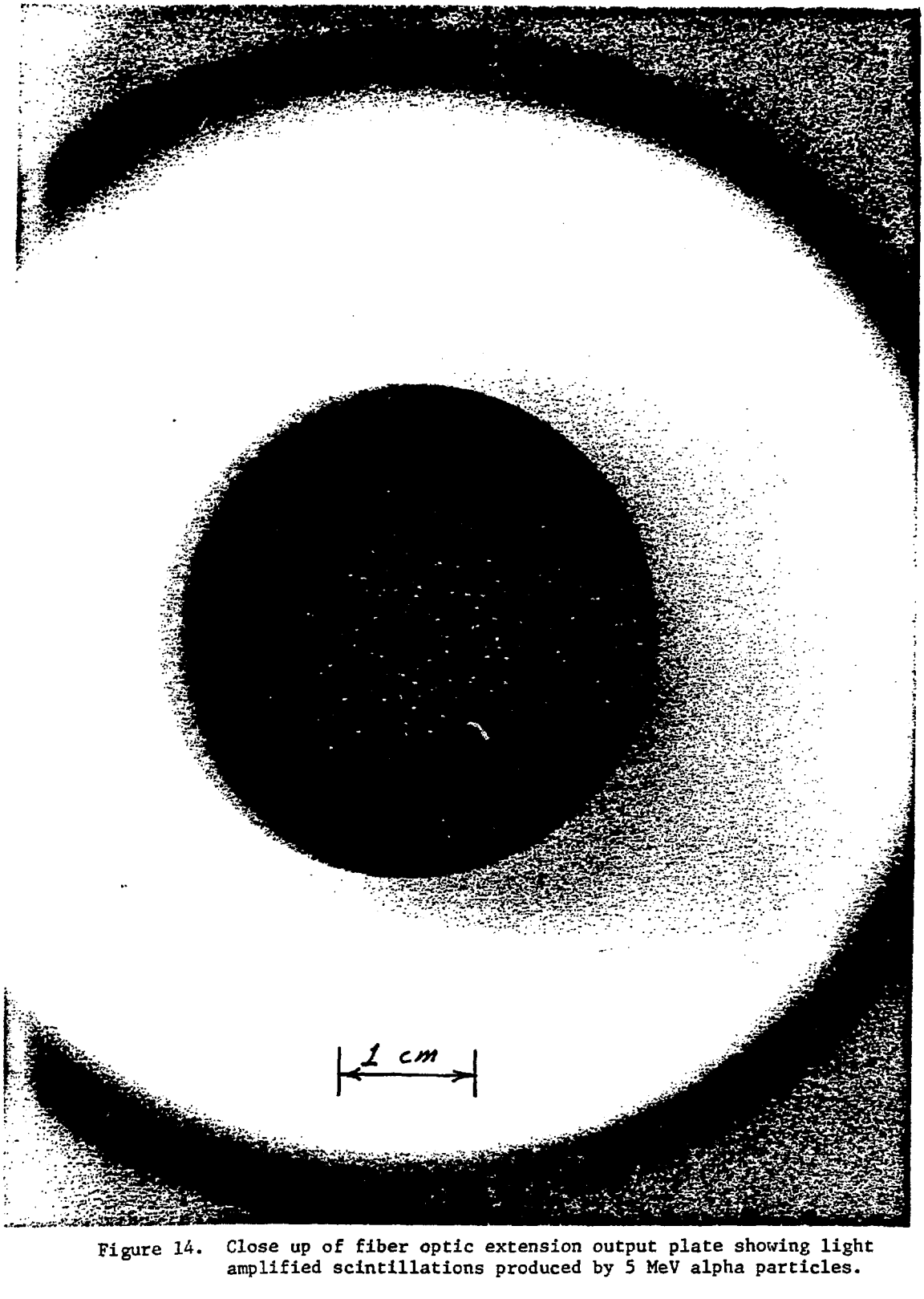

Figure 14. Close up of fiber optic extension output plate showing light amplified scintillations produced by 5 MeV alpha particles.

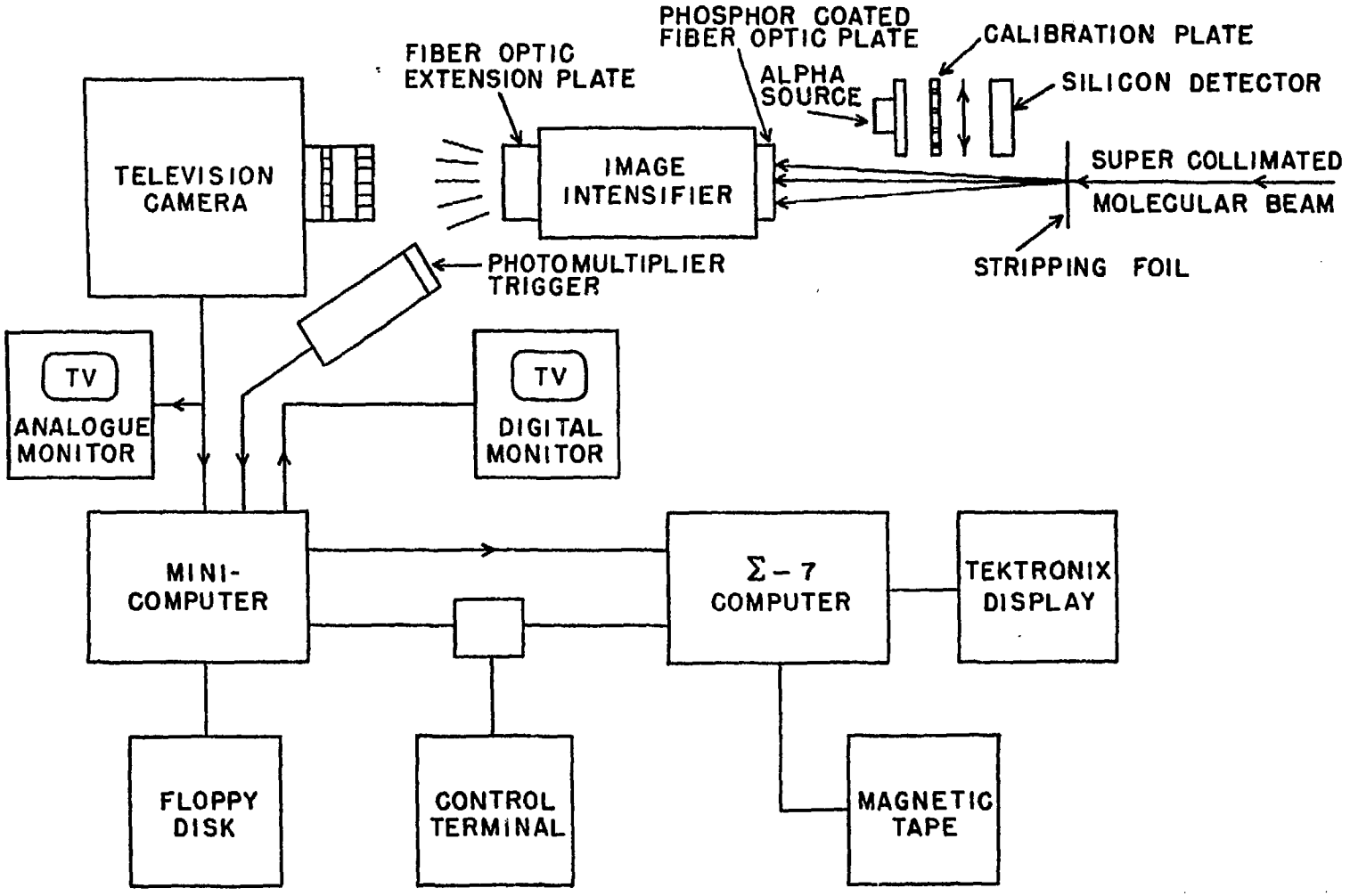

Figure 15. Schematic diagram of image intensifier detector system and television readout and digitizing system (see text).

of known spacing can also be inserted between the stripping foil and the scintillation screen in order to provide an absolute calibration of the angular spread of the Coulomb-exploded molecular ion components. The hole pattern also provides a correction matrix that could be used by the computer to correct for the slight pin cushion distortion of the image intensifier.

A television camera equipped with a high sensitivity television tube[8] and camera lens of up to F/0.95 aperture, views the 25-mm diameter output fibre optics with magnification arranged to fill most of the vertical dimension of a conventional television monitor. A small photomultiplier tube adjacent to and off-axis from the camera lens is also exposed to the amplified scintillation light and provides fast trigger signals that can be used by the logic of the television digitization system.

A photograph of the assembled apparatus is shown in Fig. 16. The television image is displayed on the monitor in the foreground and the output fibre optic plate can be seen in the middle of the picture corresponding to Fig. 14. The image intensifier housing is attached to a standard beam transport "T" fitting which includes the insertable alpha source and also the calibration plate as indicated in the schematic of Fig. 15. The next "T" section down the line contains the stripping foil and monitor detector followed by various miscellaneous beam transport components including the cryopump used to maintain the vacuum at 5×10^{-7} torr.

A commercially available television digitizing system based on a Z80 microprocessor[9] is used to digitize the scintillation light images provided by the television camera. This unit has a 64-K byte memory and two 8-inch floppy discs for system programs and data storage. The system digitizes the camera video signal continuously. The digitization is 128 horizontal by 256 vertical pixels

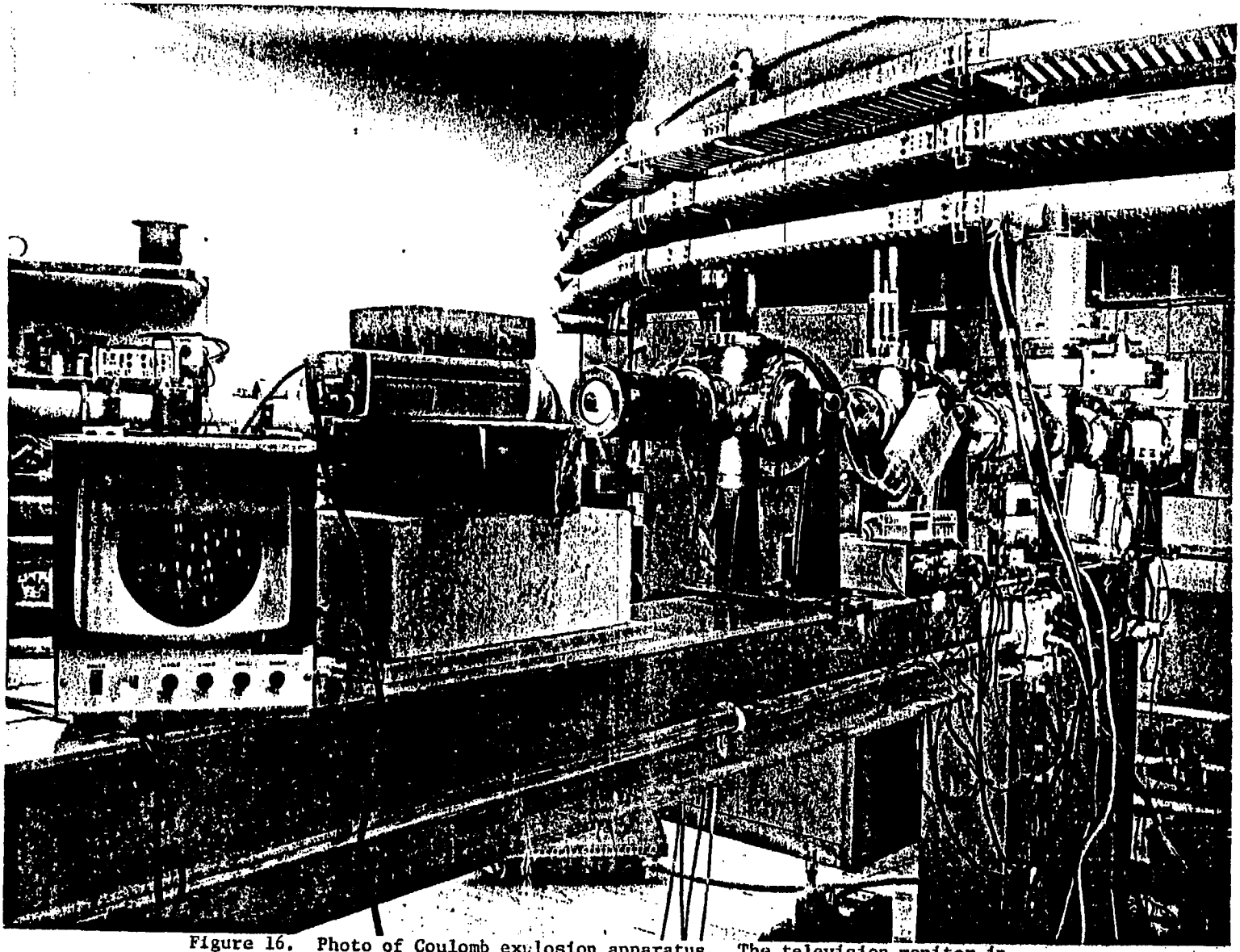

Figure 16. Photo of Coulomb explosion apparatus. The television monitor in the foreground is displaying an image of the fiber optic extension output plate of the image intensifier which in turn is showing light amplified scintillations of 5 MeV alpha particles as in Fig. 14.

so that two sequential stored frames utilize 32 K of memory. The intensity in each pixel is digitized to a 4-bit level. The control program is arranged so that if a trigger pulse from the photomultiplier occurs during a frame scan, that frame is stored and the next frame as well, providing a second trigger pulse has not occurred before the end of the second frame. By storing two frames after the trigger pulse, the system guarantees that all of the area has been scanned even though a portion of the asynchronous event could easily have occurred after the first frame scan has passed that area of the screen. The two frames are averaged and all pixels with intensity levels above a pre-set background level are stored in memory in terms of their X-Y coordinates and intensity level. When the buffer store in memory is full, it transfers onto a floppy disc which can later be read into a file of an XDS Sigma 7 computer for further analysis. The software is conveniently arranged to allow live monitoring of the events that are being stored as well as step-by-step event control.

Typical Coulomb explosion events for 4.67 MeV C_3^- molecules are shown in Fig. 17 which are plots from a Tektronix display of the digitized data. The scale corresponds to the actual distance on the scintillation screen in millimeters and the corresponding angular spread in milliradians. The system can detect carbon ions down to at least 300 keV in energy.

Figure 18 shows similar plots for $C_{4,5,6}^-$ events that indicate some of the different kinds of patterns that are observed from the Coulomb explosion of these complex ions. The patterns for display in Fig. 18 were selected because of their interesting similarities from one species of molecule to the other. However, it was interesting to note that there seemed to be definite ratios of one kind of pattern in respect to another kind and a comparison of these ratios to the ratios predicted from some particular model that is Coulomb-exploded may be the means of

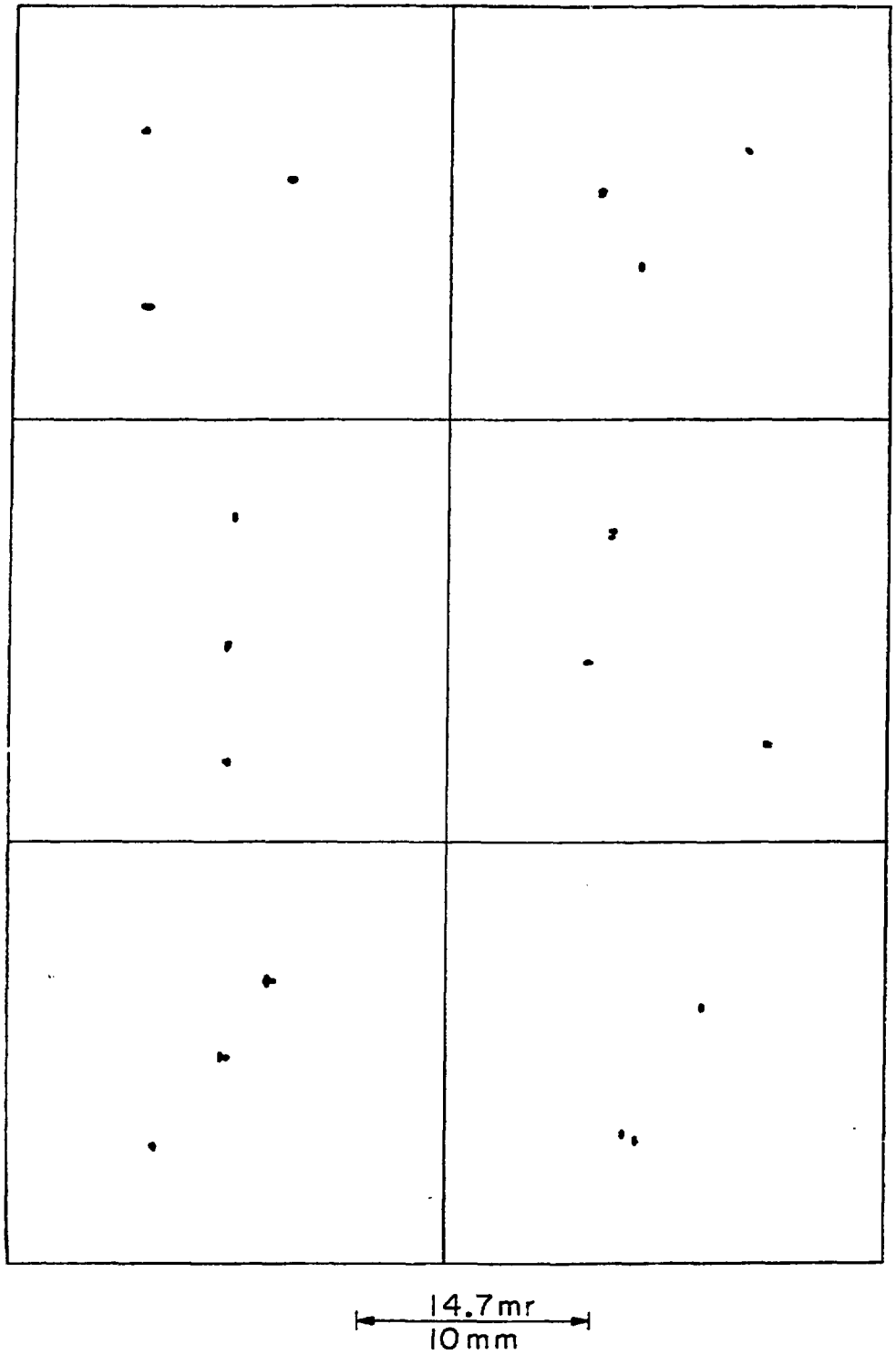

Figure 17. Typical C_3^- Coulomb explosion data as plotted from a Tektronix display.

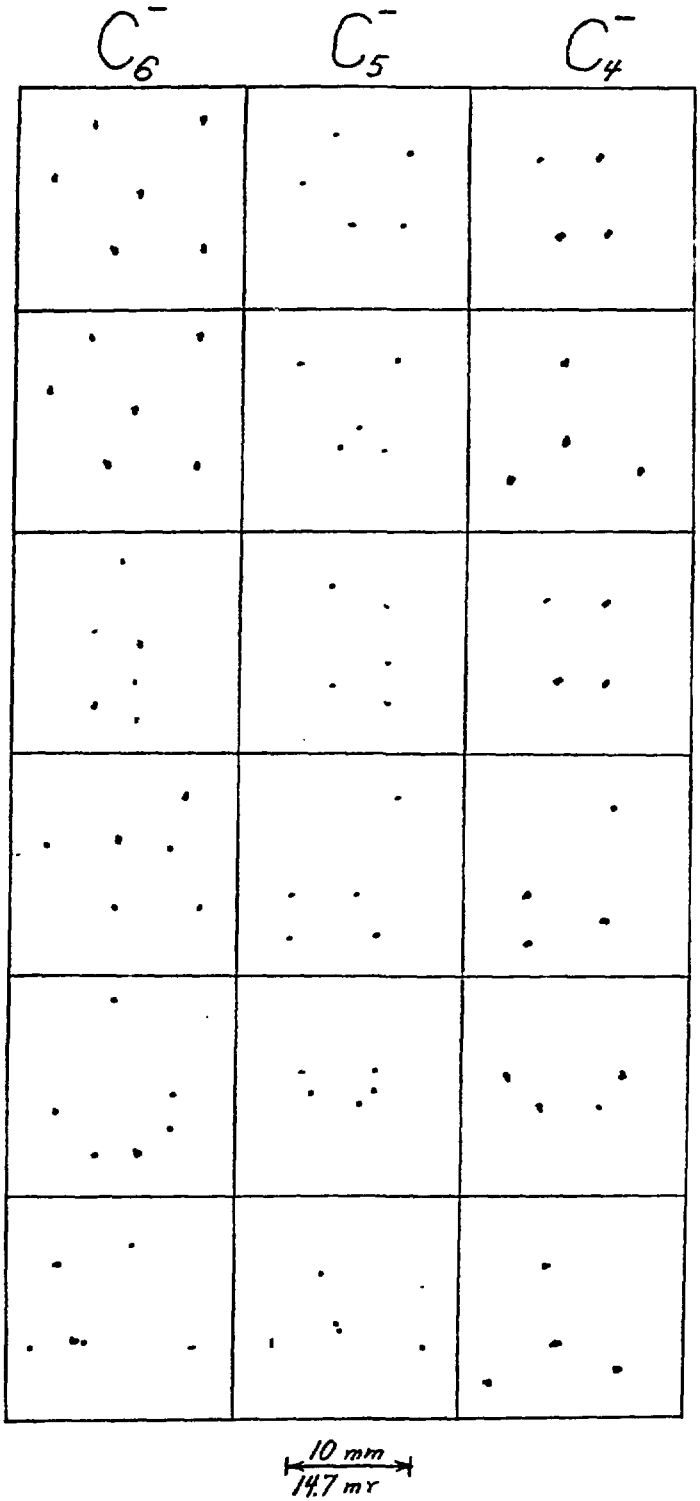

Figure 18. Typical $C^-_{4,5,6}$ Coulomb explosion data as plotted from a Tektronix display.

identifying one kind of structure from another. So far little thought has gone into what analytical method might be used for the study of these more complex systems. A further complication is that these complex molecules may have several different kinds of structures which could also confuse the final results.

III. C_2^- Explosion Analysis

The simplest carbon molecule that can be studied is the C_2^- or C_2^+ structure. The first C_2^- measurement was made with the image intensification television system and is shown in Fig. 19. This early data is being shown only because it exhibited a second experimental peak corresponding to a very small separation of Coulomb exploded events or a very large separation of the initial C_2^- molecule. The solid line through the data points is a theoretical fit assuming a rigid C_2^- dumbell structure and the known charge state distribution. A direct measure of the multiple scattering of 3.5 MeV C^- ions is included for comparison to show to what extent any structural properties of the data would be relevant in terms of the multiple scattering. The extra peak does not have to do with various charge states of the carbon atoms after the explosion and at present there is no explanation. A similar measurement with much better statistics is shown in Fig. 20 and the previously observed second peak has disappeared. It has also been observed in some very recent measurements, since those shown in Figs. 19 and 20, that the pronounced second peak has not reappeared which means that the second peak in Fig. 19 may be some kind of experimental error and not relative to the C_2^- structure.

The two fitted curves are for two different atomic spacings and two slightly different multiple scatterings. In this case the data were analyzed with the computer system which provided a distribution of the centroid of each of the Coulomb exploded events and is plotted for comparison. This distribution also indicates

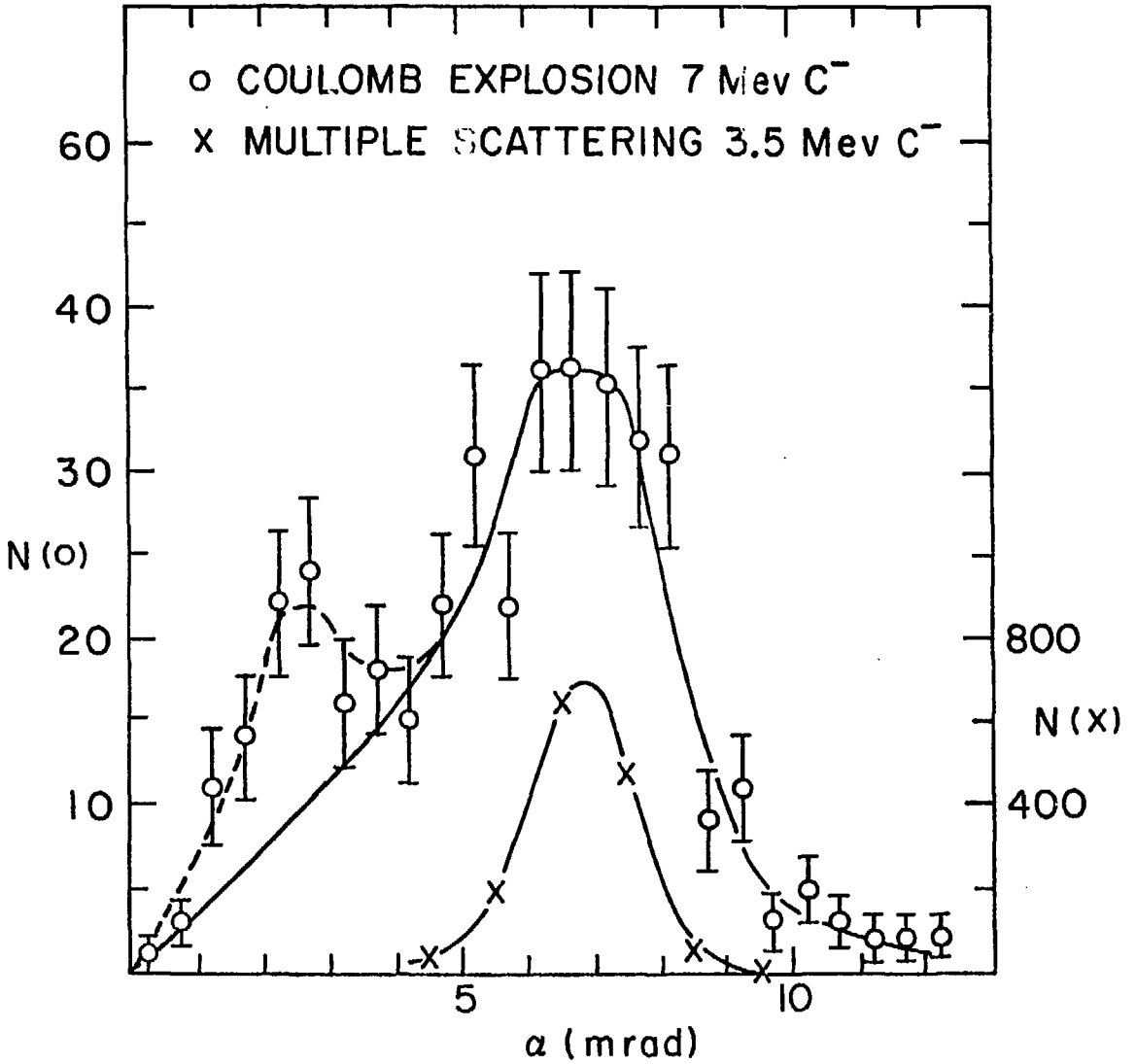

Figure 19. Experimental distribution of 7.00 MeV C_2^- Coulomb explosion events and theoretical fit (solid line through data points).

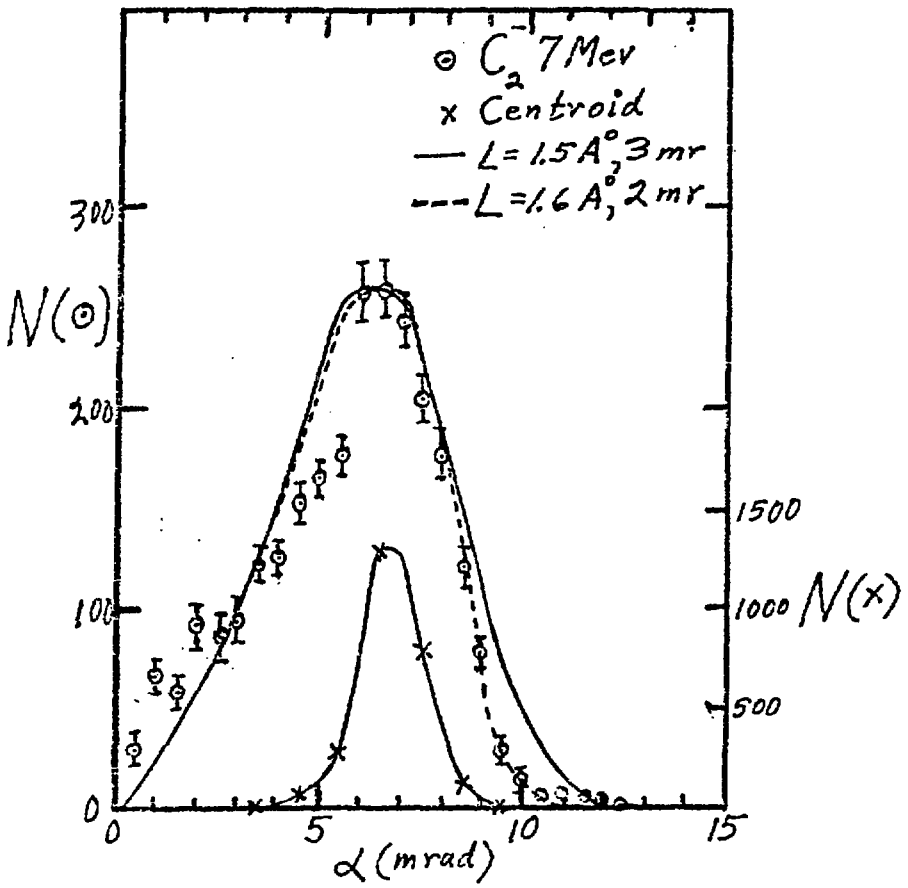

Figure 20. Improved statistics for C_2^- Coulomb explosion events fitted with different initial atomic spacings and multiple scattering.

to what degree any kind of structural properties would be relevant in terms of the multiple Coulomb scattering of both of the components of the C_2^- ion. Further measurements of C_2^- and C_2^+ systems are currently underway and much better statistics will be obtained for both of these two systems in order to determine the effective temperature of the C_2^- system when it is sputtered out of the graphite matrix.

IV. Triatomic Systems

Preliminary data taken with the new image intensifier detector system are shown in fig. 21 for C_3^-, C_3^+, and NCO^+ molecular ions. The main point to this figure is that the general distribution of events for the different molecular ions in the l vs. d/l plane is very similar except for gross properties like a shift of the centroid of the data to higher or lower l, as noted in the comparison of the C_3^+ distribution to the NCO^+ distribution. A more detailed comparison of these data can be made by projecting all of the data onto the l axis in order to show more quantitatively what the relative centroid and shape differences might be. Figure 22 is a projection of the C_3^- and C_3^+ data and shows that there is a definite shift of the centroid to larger l for the C_3^- as compared to C_3^+ events. This means that the C_3^- ion must be more tightly bound than the C_3^+ molecular ion because it has Coulomb exploded with slightly more energy as indicated by the offset.

A theoretical comparison predicting this kind of distribution from the explosion of a triangular structure is shown in Fig. 23 and indicates an offset approximately equivalent to that observed experimentally in Fig. 22. This infers that a difference in atomic spacing of 0.4 A.$^\circ$ could account for the differences between the two molecules, providing that they are triangular structures, which has not yet been proven, as compared to the possibilities of their being a flexible or

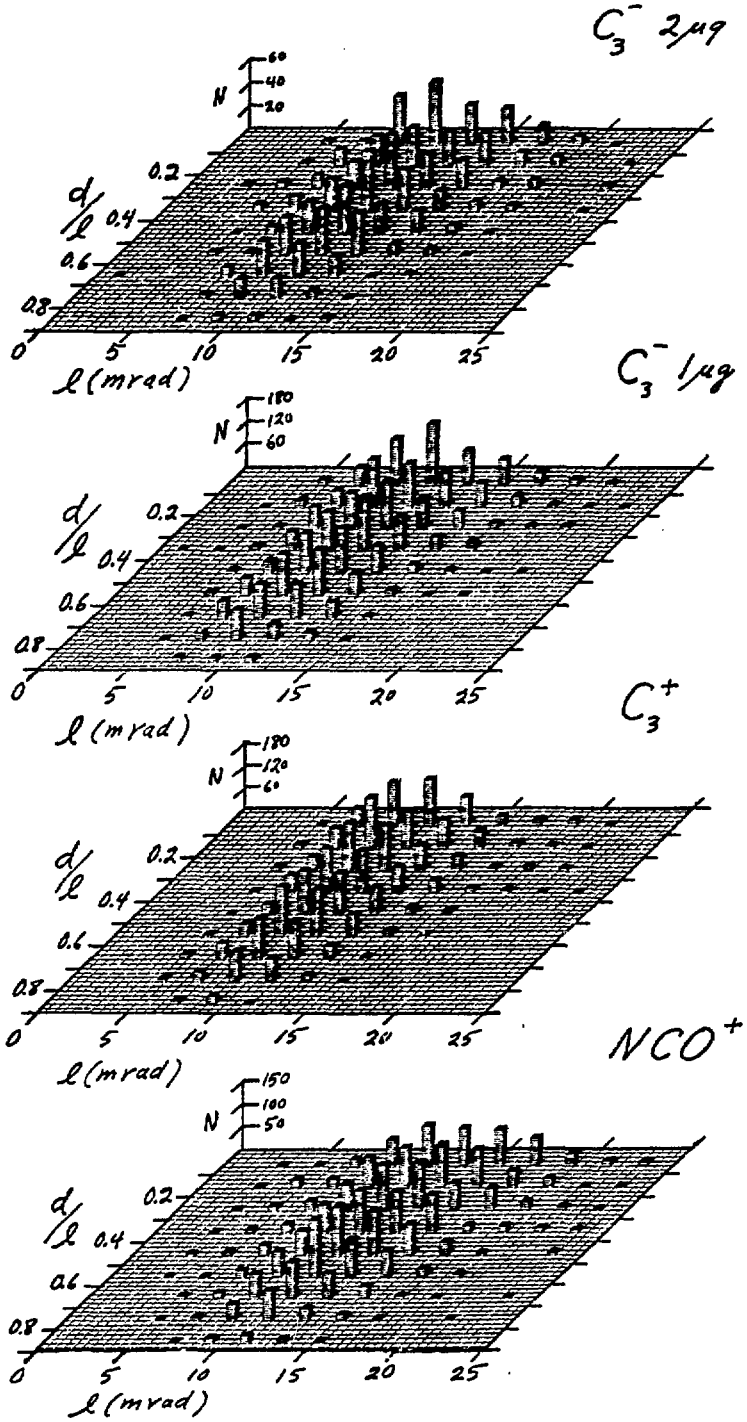

Figure 21. Comparison of C_3^+, $^-$ and NCO^+ d/l vs l distributions.

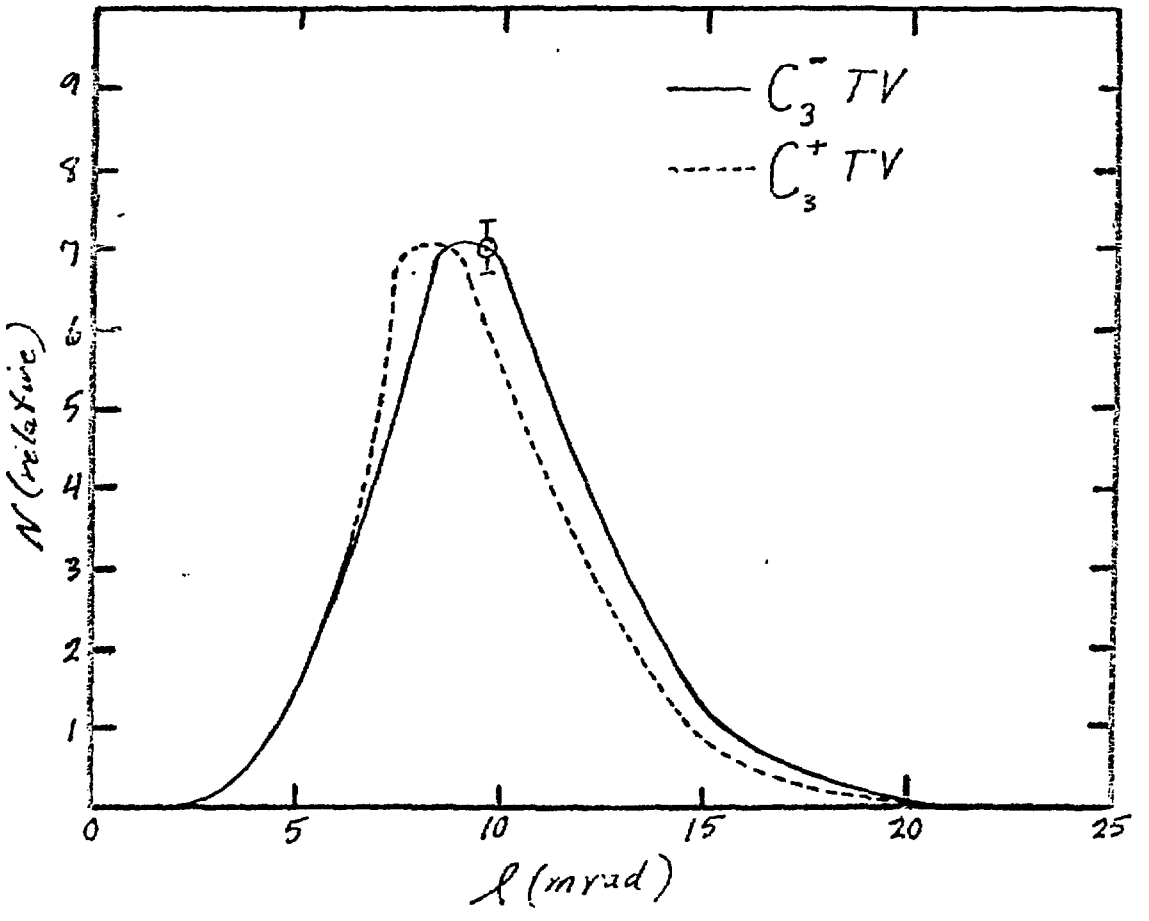

Figure 22. Distributions corresponding to the projection of all events in Figure 21 onto the 1 axis for $C_3^{+,-}$.

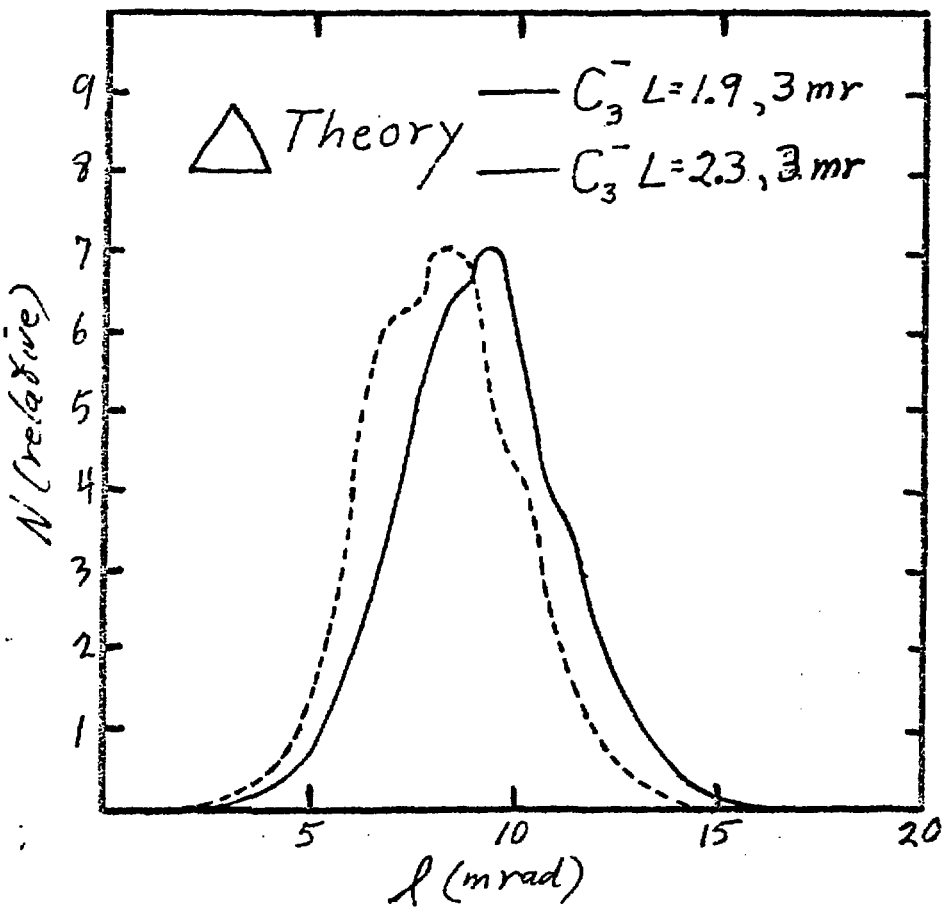

Figure 23. Theoretical distributions corresponding to a triangular structured C_3^- molecules. (Simulating Figure 22 and showing the centroid shift corresponding to an increase of 0.4 A° in the initial atomic spacing).

floppy rod-like structure. In any event, this kind of calculation shows the sensitivity of this kind of measurement for the study of some of the basic properties of these molecules through the Coulomb explosion technique.

Figure 24 is a comparison of the NCO^- and NCO^+ molecules and shows that there is little difference between these two molecules; however, there is a marked difference between the separation of atomic components when compared to the C_3^- molecule. The shift in the centroid is approximately 1 mr over that corresponding to C_3^-.

V. Multiple Scattering Anomaly

The image intensifier electronic detection system always includes as part of the analysis of the data a distribution of the centroids corresponding to each of the Coulomb explosion events. It was observed that the centroid distribution of the Coulomb explosion events indicates that the atomic constituents are scattered more than what might be expected in terms of multiple scattering of atomic ions of the same velocity. Figure 25 shows this situation for 1.56 MeV carbon ions corresponding to the carbon ion from the Coulomb explosion of 4.67 MeV C_3^- ions. The figure shows the importance of using as thin a foil as possible in comparing the 1 and 2 ug multiple scatterings and also the fact that the centroid distribution of the C_3^- events is almost identical to that measured for 1.56 MeV C^- ions. The predicted distribution is shown by the dashed lines, which indicates that an as of yet unexplained cluster efffect is going on during the molecular penetration through the foil that enhances the multiple scattering effects as observed. Table 1 is a summary of all the measurements indicating the full width at half maximum (FWHM) of the measured distributions of the centroids compared to what might be expected in terms of direct multiple Coulomb scattering measurements of the corresponding atoms. In all cases, the centroid distributions

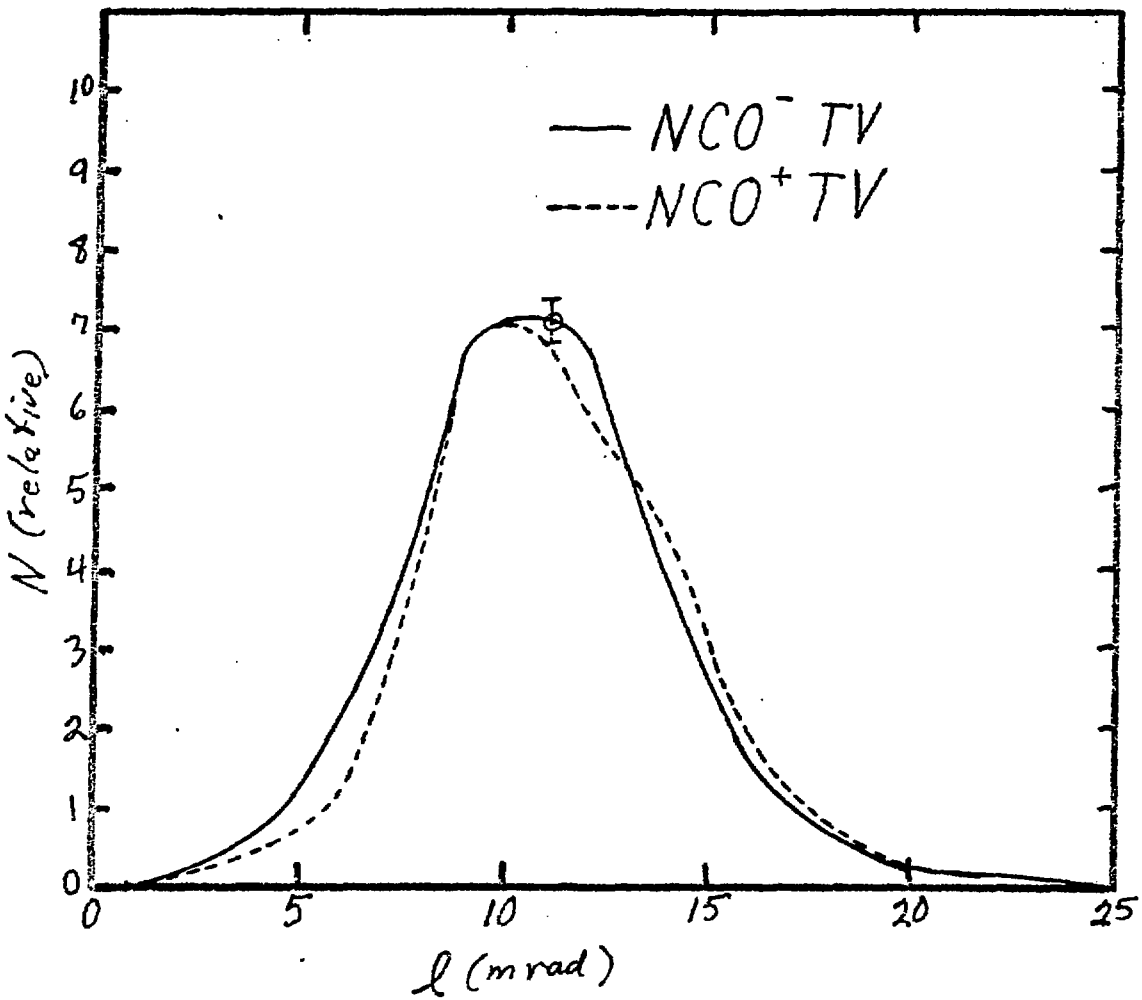

Figure 24. Distributions corresponding to the projection of all events onto the l axis for $NCO^{-,+}$.

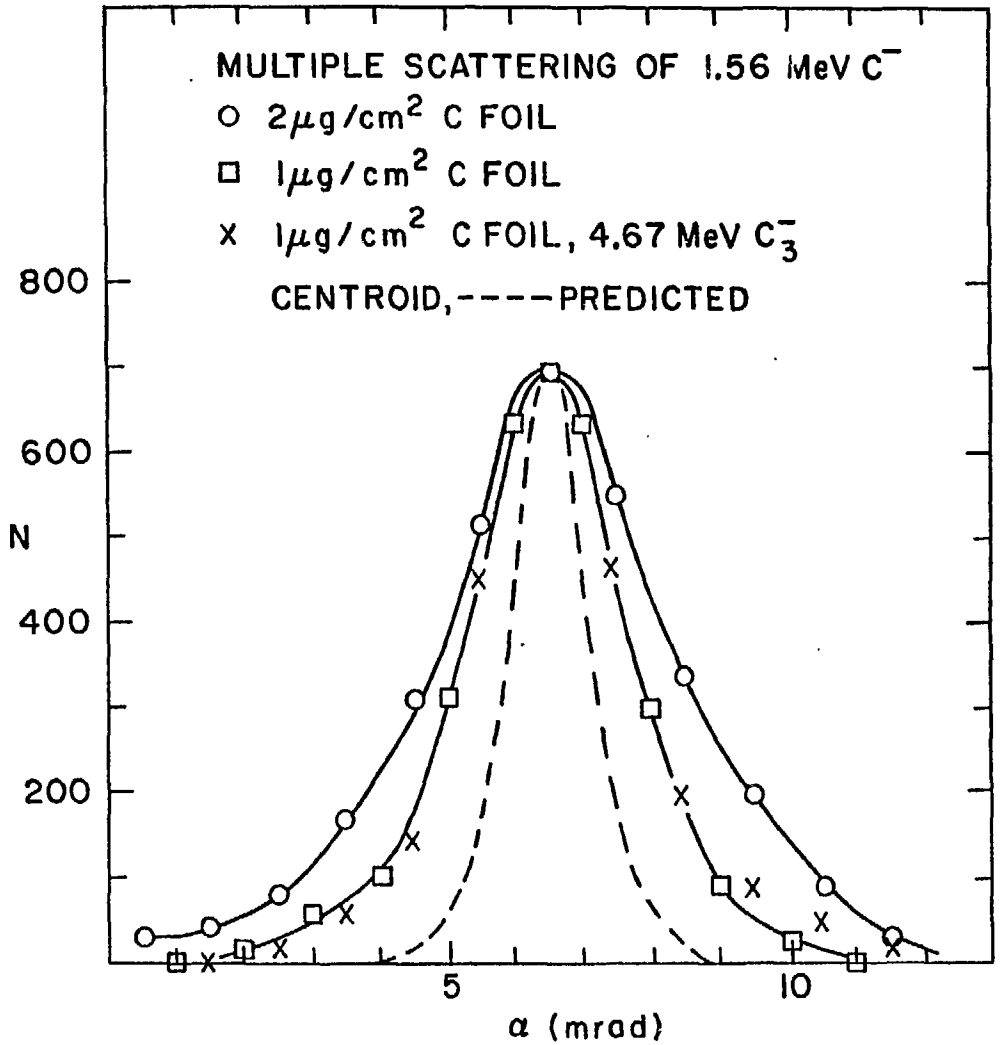

Figure 25. Comparison of multiple scattering of 1.56 MeV C^- ions and the centroid of Coulomb exploded 4.67 MeV C_3^- ions.

TABLE I

Summary of Coulomb Explosion Centroid and Carbon Ion Multiple Scattering Widths (FWHM)

Run #	E/A keV/AMU	ugm/cm^2	Δx mrad	Δy mrad	Average mrad	Expected (gaussian)
C-Run 2	130	2	3.0	3.75	3.38	
C3-R1	130	2	3.52	3.31	3.42	1.95
C-R1-1	130	1	1.90	2.59	2.24	
C3+R1-1	130	1	2.25	2.53	2.39	1.29
C3-R1-26	130	1	2.41	2.65	2.53	1.29
C-R1-26	292	1	1.82	1.71	1.76	
C2-R1-26	292	1	1.54	1.69	1.62	1.24
CNO+R1-1	95	1	2.92	2.98	2.95	
NCO-2-15	95	1	2.70	--		

are noticeably wider than what would be expected in terms of simple Coulomb scattering.

VI. Summary

In summary, this new image intensifier detector system, coupled with a microcomputer, has proven to be a valuable tool in the study of the Coulomb explosion of complex molecules that penetrate matter. In the future, with some additional improvements in the system, and much better statistics for most of the molecules studied to date, it is expected that much new information will be gained about the structure of many kinds of complex molecular ions including the special effects that may be encountered when these fast molecular ions penetrate matter.

REFERENCES

1. Hiconex Model 832 Cs-Ion source manufactured by the General Ionex Corp., 19 Gras Rd., Newburyport, MA. 01950.

2. Ryoichi Hayatsu, Robert G. Scott and Martin H. Studier, Science 209, 1512-17 (1980).

3. Goldring, G., Eisen, Y., Thieberger, P., Wegner, H.E., and Filevich, A., C_3^- + A NCO Molecular Ion Structure Studies by Coulomb Explosion. Phys. Rev. (Submitted), Bull. Am. Phys. Soc. 26, 48 (1981).

4. Wegner, H. E., and Thieberger, P. Molecular Explosion of Large Penetrating Clusters. Proceedings of the Informal Workshop on the Penetration of Exotic Particles in Matter, New York University, New York, January 8-11, 1981 (in press): G. Goldring, P. Thieberger and H. E. Wegner, Molecular Structure Information from the Coulomb 6 Explosion of C_3^- and C_3^+ Ions, Israeli Annals of Physics (in press).

5. Thieberger, P., and Wegner, H.E. 2D Multiple Event Image Intensifier Scintillation Ion Detector. Bull. Am. Phys. Soc. 26, 46 (1981); Israeli Annals of Physics (in press), Nucl. Instrum. & Methods (submitted).

6. Grant Scientific Co., P.O. Box 11729, Columbia, South Carolina 29211.

7. Model No. 1122 Varo Electron Devices, Inc., 2203 West Walnut Street, P.O. Box 401146, Garland, Texas 75040.

8. Newvicon, Type S4075; Panasonic Electronic Components Division, One Panasonic Way, Secaucus, New Jersey 07094.

9. Tecmar Inc., 23414 Greenlawn, Cleveland, Ohio 44122.